ORIGINAL ARTICLE

Cancer Science WILEY

Oncogenic LINC00857 recruits TFAP2C to elevate FAT1 expression in gastric cancer

Wenqing Zhang[1] | Kaiyue Ji[1] | Congcong Min[2] | Cuiping Zhang[1] | Lin Yang[1] | Qi Zhang[1] | Zibin Tian[1] | Mengyuan Zhang[1] | Xinyu Wang[1] | Xiaoyu Li[1] (iD)

[1]Department of Gastroenterology, The Affiliated Hospital of Qingdao University, Qingdao, China

[2]Hospital of Qingdao University, Qingdao, China

Correspondence
Xiaoyu Li, Department of Gastroenterology, The Affiliated Hospital of Qingdao University, No. 16, Jiangsu Road, Qingdao 266000, Shandong Province, China.
Email: lixiaoyu05@163.com

Abstract

FAT atypical cadherin 1 (FAT1) is a mutant gene frequently found in human cancers and mainly accumulates at the plasma membrane of cancer cells. Emerging evidence has implicated FAT1 in the progression of gastric cancer (GC). This study intended to identify a regulatory network related to FAT1 in GC development. Upregulated expression of FAT1 was confirmed in GC tissues, and silencing FAT1 was observed to result in suppression of GC cell oncogenic phenotypes. Mechanistic investigation results demonstrated that FAT1 upregulated AP-1 expression by phosphorylating c-JUN and c-FOS, whereas LINC00857 elevated the expression of FAT1 by recruiting a transcription factor TFAP2C. Functional experiments further suggested that LINC00857 enhanced the malignant biological characteristics of GC cells through TFAP2C-mediated promotion of FAT1. More importantly, LINC00857 silencing delayed the tumor growth and blocked epithelial–mesenchymal transition in tumor-bearing mice, which was associated with downregulated expression of TFAP2C/FAT1. To conclude, LINC00857 plays an oncogenic role in GC through regulating the TFAP2C/FAT1/AP-1 axis. Therefore, this study contributes to extended the understanding of gastric carcinogenesis and LINC00857 may serve as a therapeutic target for GC.

KEYWORDS
AP-1, FAT1, gastric cancer, invasion, LINC00857, migration, proliferation, TFAP2C

1 | INTRODUCTION

Gastric cancer remains one of the most prevalent malignant tumors associated with high mortality and imposes high global disease burden.[1] It is the fifth most frequently occurring malignancy and the third most common death-related cause of cancer on a global basis.[2] GC is considered as the most common cancer diagnosed in both males and females in China and accounts for 57% of cancers diagnosed in China.[3] The investigations of molecular and clinical characteristics of GC have been complicated due to heterogeneous histologic and etiologic properties.[4]

Emerging evidence has indicated the active role of lncRNAs in tumorigenesis, metastasis, drug resistance, and prognosis of GC through several molecular mechanisms.[5] LINC00857 as a

---

upregulated lncRNA in GC tissues relative to adjacent normal tissues, has been demonstrated as a potential marker for GC diagnosis in the initial discovery phase.[6] Bioinformatics analysis using the RPISeq database suggested an interaction between LINC00857 and transcription factor activating protein 2 gamma (TFAP2C), which is a transcription factor of the AP2 family, and is upregulated during the transition from primed to naive, being widespread at the naive-specific enhancer.[7] TFAP2C has been reported to associate with the super-enhancer in GC.[8] In addition, amplified TFAP2C expression links to advanced clinicopathological characteristics, poor prognosis, and accelerated disease progression in colorectal cancer, another kind of gastrointestinal cancer.[9]

Of note, our bioinformatics analysis based on the JASPAR database indicated putative regulation of TFAP2C to FAT1. FAT1 is a cellular factor functioning as a driver of gastric carcinogenesis, the mRNA of which has been expressed in embryonic stem cells, neural tissues, GC, colorectal cancer, pancreatic cancer, lung cancer, breast cancer, and brain tumors.[10] FAT1 represents an adhesion molecule promoting cell invasion; its silencing by the drug verteporfin can suppress the metastatic potential of GC, and therefore may serve as a promising therapeutic strategy against GC.[11] FAT1 acts as an upstream regulator of the transcription factor AP-1, then affecting the oncogenic and inflammatory pathways in glioma cells.[12] The reduced activity of AP-1 contributes to the suppression of GC cell proliferation and invasion ability as well as slowed tumor growth.[13] Here, our study was conducted to determine the network among LINC00857, TFAP2C, FAT1, and AP-1 signaling, and to testify if the aforementioned network was involved in the carcinogenesis of GC.

2 | MATERIALS AND METHODS

2.1 | Ethics statement

The current study was performed with the approval of the ethics committee of the Affiliated Hospital of Qingdao University and performed in strict accordance with the *Declaration of Helsinki*. All participants or legal guardians signed informed consent documentation. Animal experiments were approved by the ethics committee of the Affiliated Hospital of Qingdao University and strictly adhered to the principles to minimize the pain, suffering, and discomfort to experimental animals.

2.2 | Clinical sample collection

In total, 46 patients with GC who underwent surgery at the Affiliated Hospital of Qingdao University from May 2012 to December 2014 were enrolled in the current study. GC and adjacent normal tissue specimens were obtained and pathologically diagnosed. Classification and tumor staging were conducted based on the criteria established by the WHO (2010) and UICC/AJCC TNM classification (7th edition) along with Lauren's classification (intestinal/diffused GC).[14] The basic information of patients was collected from the medical record room, and all patients were followed up to collect the clinical outcome information after treatment. The Kaplan–Meier method was used to analyze the relationship between FAT1 expression and OS.

2.3 | Cell culture and treatment

GC cell lines of HGC27, MKN45 and normal gastric epithelial cells GES-1 were acquired from Procell Life Science & Technology. These cells were cultured in RPMI 1640 medium supplemented with 10% FBS (Gibco), 10 μg/ml streptomycin and 100 U/ml penicillin (Gibco) at 37°C, in 5% CO_2.

Cells were then transduced with lentivirus expressing shRNA carrying sequences targeting FAT1 (sh-FAT1-1, sh-FAT1-2) TFAP2C (sh-TFAP2C), or LINC00857 (sh-LINC00857), or lentivirus overexpressing them (oe-FAT1, oe-TFAP2C, oe-LINC00857), or the corresponding negative control (sh-NC, oe-NC). All lentivirus were synthesized by Shanghai Heyuan Biotechnology at a titer of 1×10^7–1×10^8. For transduction, cells in the logarithmic phase of growth were seeded onto six-well plates (2×10^5 cells/well). Upon reaching a cell confluency of 60%, 800 μl fresh virus solution was mixed with 800 μl FBS and added with Polybrene to a final concentration of 6 μg/ml, followed by incubation with the cells for 12–24 h. The culture medium was then replaced by complete medium, at which time cells were further cultured at 37°C in 5% CO_2. After 48 h of transduction, 2.5 μg/ml puromycin was used to screen cells for 7–10 days, followed by RT-qPCR and western blot analyses to verify successful transduction.

2.4 | RNA extraction and quantification

Total RNA was extracted from cells using TRIzol reagent (15596026, Invitrogen) and subjected to reverse transcription using the Prime Script RT reagent kit (RR047A) to obtain cDNA. RT-qPCR was then performed with the use of an ABI PRISM 7500 instrument (Applied Biosystems) and the Fast SYBR Green PCR kit (Applied Biosystems), with three duplicate well sets for each sample. Primers used in the assay are listed in Table S1. GAPDH was used as an internal reference, and the relative mRNA expression of tested genes was calculated using the $2^{-\Delta\Delta C_t}$ method.

2.5 | Western blot analysis

Total protein of cells was extracted using RIPA lysis buffer containing protease inhibitors and phosphatase inhibitors, and the protein concentration was then quantified using a bicinchoninic acid protein assay kit. Next, the protein was separated by 10% sodium dodecyl sulfate-polyacrylamide gel electrophoresis and electro-transferred

onto polyvinylidene fluoride membranes. The membrane was blocked with 5% bovine serum albumin (BSA) at room temperature for 2h and probed overnight at 4°C with primary antibodies to TFAP2C (rabbit, ab76007, 1:10,000), FAT1 (mouse, ab14381, 1:1000), N-cadherin (rabbit, ab76011, 1:1000), p-JUN (rabbit, ab227533, 1:1000); c-Jun (rabbit, ab40766, 1:1000), p-FOS (rabbit, ab222699, 1:1000), c-FOS (mouse, ab208942, 1:1000), AP-1 (rabbit, ab230273, 1:1000), E-cadherin (rabbit, ab40772, 1:10,000), vimentin (rabbit, ab92547, 1:1000), MMP2 (rabbit, ab92536, 1:1000) MMP9 (rabbit, ab76003, 1:1000), and β-actin (mouse, ab8226, 1:10,000). Afterward, the membrane was re-probed with the horseradish peroxidase-conjugated secondary goat anti-rabbit IgG (ab205719, 1:2000, Abcam Inc.) or goat anti-mouse (ab97035, 1:2000, Abcam Inc.) for 1h at room temperature. The blots were visualized using ECL reagent, followed by exposure to X-ray film. With β-actin as the internal reference, the band intensity was quantified using ImageJ 1.48 software.

2.6 | FISH assay and immunofluorescence staining

The subcellular localization of LINC00857 was identified using the Ribo™ lncRNA FISH Probe Mix (Red). HGC-27, MKN-45 and GES-1 cells were seeded into six-well culture plates (1×10^5 cells/well). Upon reaching ~80% cell confluence, the slides were fixed with 4% paraformaldehyde. and treated successively with proteinase K (2 μg/ml), glycine, and acetamidine reagent, followed by the addition of prehybridization solution (250 μl) and a 1-h incubation at 42°C. Then, cells were incubated overnight with hybridization solution (250 μl) containing the probe (300 ng/ml) overnight at 42°C. After PBST washing, slides were permeabilized with 0.3% Triton X-100, allowed to stand at room temperature for 30 min, blocked with goat serum, and incubated overnight with primary antibody against TFAP2C (1:200, ab110635, Abcam), followed by a 1-h incubation with secondary antibody (1:200, ab150115, Abcam). Next, DAPI (1:800) dye solution was added to stain the nucleus, and the cell slides were mounted using an anti-fluorescence quencher. A fluorescence microscope (Olympus Optical) was used for microscope observation, in which five different visual fields were randomly selected for each slide.

2.7 | RNA binding protein immunoprecipitation

Binding of LINC00857 to TFAP2C protein was measured using the MagNA RIP kit (Millipore). Cells were lysed on ice for 5 min with RIPA lysis buffer, followed by a 10-min centrifugation (7000 g, 4°C), and the supernatant was harvested. Next, with a portion of cell extract as input, the remaining was incubated with antibody for co-precipitation. Briefly, 50 μl magnetic beads of each co-precipitation reaction system was extracted and incubated with 5 μg antibody, after which the magnetic bead–antibody complex was resuspended

in RIP Wash Buffer (900 μl) and then incubated overnight at 4°C with cell extract (100 μl). Thereafter, the bead–protein complex was separated. The samples and input were detached using protease K, and the RNA was then extracted for subsequent RT-qPCR measurement. The antibody used in this assay included rabbit antibody against TFAP2C (ab76007, 1:500, Abcam Inc.) and goat anti-human IgG (ab109489, 1:100, Abcam Inc.) as the NC.

2.8 | RNA pull-down assay

GC cells were transfected with 50 nM biotin-labeled (Bio)-LINC00857-wild type (Wt) and Bio-LINC00857-mutant (Mut) (Wuhan GeneCreate Biological Engineering). After 48h, cells were harvested, incubated for 10 min in lysis buffer (Ambion). After that, the lysate was incubated with M-280 streptavidin magnetic bead (Sigma) pre-coated with RNase-free BSA and yeast tRNA at 4°C for 3h. Next, the aforementioned cell lysate and the magnetic beads were washed successively with pre-cooled lysis buffer, low salt buffer, and high salt buffer. The TFAP2C expression was examined by western blot analysis.

2.9 | Dual-luciferase reporter gene assay

The promoter fragment of FAT1 gene was amplified by PCR (as shown in Table S2). The PCR primers were synthesized by Sangon Biotech and cloned into pmirGLO vector (Promega). Wild type (Wt) and mutant (Mut) recombinant dual-luciferase reporter plasmids were constructed. 293T cells (from the ATCC) were treated with TFAP2C recombinant protein or DMSO and pmirGLO-FAT1-Wt promoter or pmirGLO-FAT1-Mut promoter. After 30h of transfection, the cells were collected. The luciferase activity was detected using a dual-luciferase reporter gene assay kit (Promega) with a Glomax 20/20 luminometer (YPH-Bio).

2.10 | Chromatin immunoprecipitation

GC cells were fixed with 1% formalin and incubated at 37°C for 10 min to produce DNA-protein cross-linking. Then, the cells were added with glycine, mixed, and allowed to stand at room temperature for 5 min to terminate the cross-linking. With the medium completely absorbed, the cells were collected in a 15-ml centrifuge tube with a cell scraper for a 5-min centrifugation (1000 g) after precooling. The supernatant was removed and cells were harvested, which were lysed by sodium dodecyl sulfate lysis buffer and subjected to ultrasonic cleavage (VCX750, 25% power, 4.5 s impact, 9 s interval, a total of 14 times). After 10-min centrifugation (10,000 g), cells were probed with the primary antibody anti-TFAP2C at 65°C for 3h to relieve cross-linking, followed by RT-qPCR measurement of precipitated DNA.

2.11 | 5-Ethynyl-2'-deoxyuridine (EdU) assay

Cells were seeded into 24-well plates, with three replicates set in each group, and incubated with EdU solution (10 μmol/L) for 2 h. The medium was removed, and cells were then incubated with PBS solution containing 4% paraformaldehyde for 30 min at room temperature. After PBS washing, cells were incubated first with PBS containing 0.5% Triton-100 for 20 min at room temperature, and then with 100 μl Apollo staining solution for 30 min in the dark. DAPI was added for 5 min for nuclear staining. Finally, 6–10 visual fields were randomly selected and observed under a fluorescence microscope (FM-600, Shanghai Pudan Optical Instrument).

2.12 | Transwell assay

Cells were resuspended in serum-free medium to a density of 2×10^4 cells/ml. Matrigel-coated Transwell chambers were used to test cell invasion, and uncoated chambers were used to examine cell migration. Next, 100 μl cell suspension was added to the upper Transwell chamber, and 700 μl medium containing 20% FBS was added in the lower chamber, followed by culture (5% CO_2, 37°C) for 12–24 h. Then, the inner membrane of the chamber was gently wiped with a cotton swab to remove the attached cells. The cells were fixed in 1% glutaraldehyde for 30 min, and stained with 0.1% crystal violet for 12 h. The number of stained cells was counted under an inverted microscope (XDS-800D, Shanghai Caikon Optical Instrument) in 6–10 randomly selected visual fields.

2.13 | GC xenografts in nude mice

Male specific pathogen-free BALB/c nude mice (aged 6 weeks old, weighing: 20–22 g) were housed under conditions of 60–65% humidity, 22 to 25°C, and a 12-h light/dark cycle, with free access to food and water. The GC HGC-27 cells stably transduced with sh-LINC00857/sh-FAT1/oe-FAT1 were obtained, 1.5 $\times 10^6$ of which were suspended in 0.1 ml serum-free medium. After a week of acclimatization, mice were grouped and subcutaneously injected on the back with the corresponding cell suspension (100 μl). Following this, the length and width of tumor xenografts were recorded every 10 days, and the tumor size was calculated using the formula: volume = 0.5 $\times$ length $\times$ width^2. After 40 days, mice were euthanized, tumor xenografts were removed, and the weight and volume were measured.

2.14 | Statistical analysis

SPSS 21.0 software (IBM Corp) was used for statistical data analyses. The measurement data were presented as mean ± standard deviation. Data between two groups were compared using independent sample t-test, whereas those among multiple groups were assessed using one-way ANOVA, followed by Tukey's post hoc test. Statistical analysis in relation to time-based measurements within each group was realized using repeated measures ANOVA with Tukey's post hoc test. A p-value < 0.05 was considered to be statistically significant.

3 | RESULTS

3.1 | FAT1, highly expressed in GC tissues and cells, is positively correlated with the pathological grade of GC patients

We first investigated FAT1 expression in tumors included in The Cancer Genome Atlas (TCGA), and found that it was increased in a variety of tumors (Figure 1A). In the GC and adjacent normal samples retrieved from TCGA and GTEx, FAT1 expression exhibited an obvious increase in GC samples (Figure 1B). In addition, the upregulated mRNA and protein levels of FAT1 were verified in clinically collected GC tissues ($n = 46$) relative to adjacent normal tissues ($n = 46$) (Figure 1C,D).

Furthermore, analysis of pathological data of the enrolled patients displayed that FAT1 expression increased as the pathological grade of GC went higher (Figure 1E). In addition, higher FAT1 expression was identified in diffused GC compared with intestinal GC (Figure 1F). It can therefore be ascertained that FAT1 expression is correlated with GC grading/classification. Analysis on open prognostic data then unveiled that the survival time of GC patients with high FAT1 expression was shorter than that of patients with low FAT1 expression (Figure 1G, $p = 0.002$), suggesting FAT1 to be a prognostic factor for GC. Furthermore, an enhancement of FAT1 expression was confirmed in GC cell lines (HGC27 and MKN-45) relative to GES-1 cells (Figure 1H,I).

These results demonstrated that the upregulation of expression of FAT1 occurred in both GC tissues and cells, which had correlations with GC pathological grading and poor prognosis.

3.2 | Knocking down FAT1 attenuates GC cell malignant behaviors in vitro and the GC cell tumorigenicity in vivo

To probe into the effect of FAT1 on the growth of GC cells, we constructed HGC27 and MKN-45 cells stably transduced with oe-FAT1 and sh-FAT1, with the transfection efficiency determined by western blot analysis and RT-qPCR. The knockdown efficiency reached more than 70% (Figure 2A,B). Subsequent Transwell assays displayed that FAT1 overexpression enhanced the proliferative, migratory and invasive properties of GC cells, whereas the opposite effects were noted in response to knockdown of FAT1
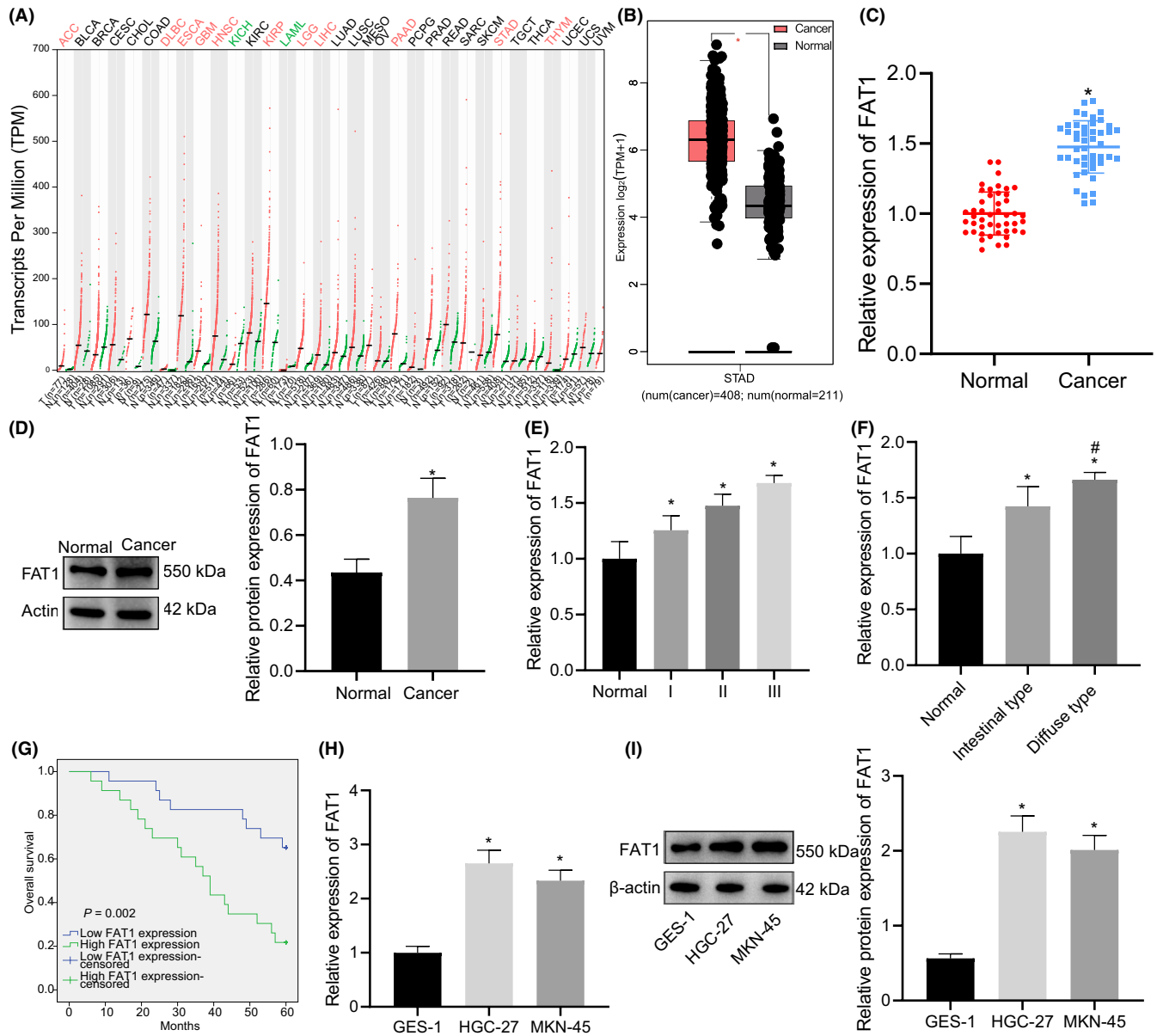
FIGURE 1 Abundant FAT1 expression in GC tissues and cells. (A) The expression of FAT1 in tumors included in TCGA. The abscissa represents the tumor and sample types, and the ordinate represents the FAT1 expression level. (B) The expression of FAT1 in GC and adjacent normal samples included in TCGA and GTEx of the GEPIA2 database (http://gepia2.cancer-pku.cn/#analysis). The abscissa represents the sample type, the ordinate represents the expression level, the red box diagram represents the GC sample, and the gray box diagram represents the adjacent normal sample (*$p < 0.01$). (C) The expression of FAT1 in GC ($n = 46$) and adjacent normal tissues ($n = 46$) determined by RT-qPCR. (D) Western blot analysis of FAT1 protein in GC ($n = 46$) and adjacent normal tissues ($n = 46$). (E) Correlation of FAT1 expression with the pathological grade of GC patients. (F) Correlation of FAT1 expression with the Lauren's classification (diffused/intestinal) of GC. (G) Curve of FAT1 expression and OS of GC patients in GC tissues ($n = 46$) analyzed by the Kaplan–Meier method. (H) The expression of FAT1 in GC cell lines (HGC-27 and MKN-45) and normal gastric epithelial cell line GES-1 determined by RT-qPCR. (I) Western blot analysis of FAT1 protein in GC cell lines (HGC-27 and MKN-45) and normal gastric epithelial cell line GES-1. Data are shown as mean ± standard deviation. Cell experiments were repeated three times. Data between GC and adjacent normal tissues were compared with paired t-test, whereas those between other two groups were compared using unpaired t-test. Data among multiple groups were analyzed by one-way ANOVA, followed by a Tukey multiple comparisons post test. *$p < 0.05$, compared with adjacent normal tissues or normal gastric epithelial cell line GES-1. #$p < 0.05$, compared with intestinal GC

(Figure 2C–E). In the tumor xenograft model in nude mice, overexpression of FAT1 potentiated the tumorigenicity of GC cells, while FAT1 knockdown decreased it (Figure 2F). Collectively, these experimental data indicated that silencing FAT1 restricted the oncogenic phenotypes of GC cells in vitro as well as the tumorigenicity of GC cells in vivo.

3.3 | FAT1 enhances the malignant characteristics of GC cells by upregulating AP-1 expression

Then we proceeded to exploit the downstream mechanism of FAT1 in the malignant progression of GC. FAT1 has previously been
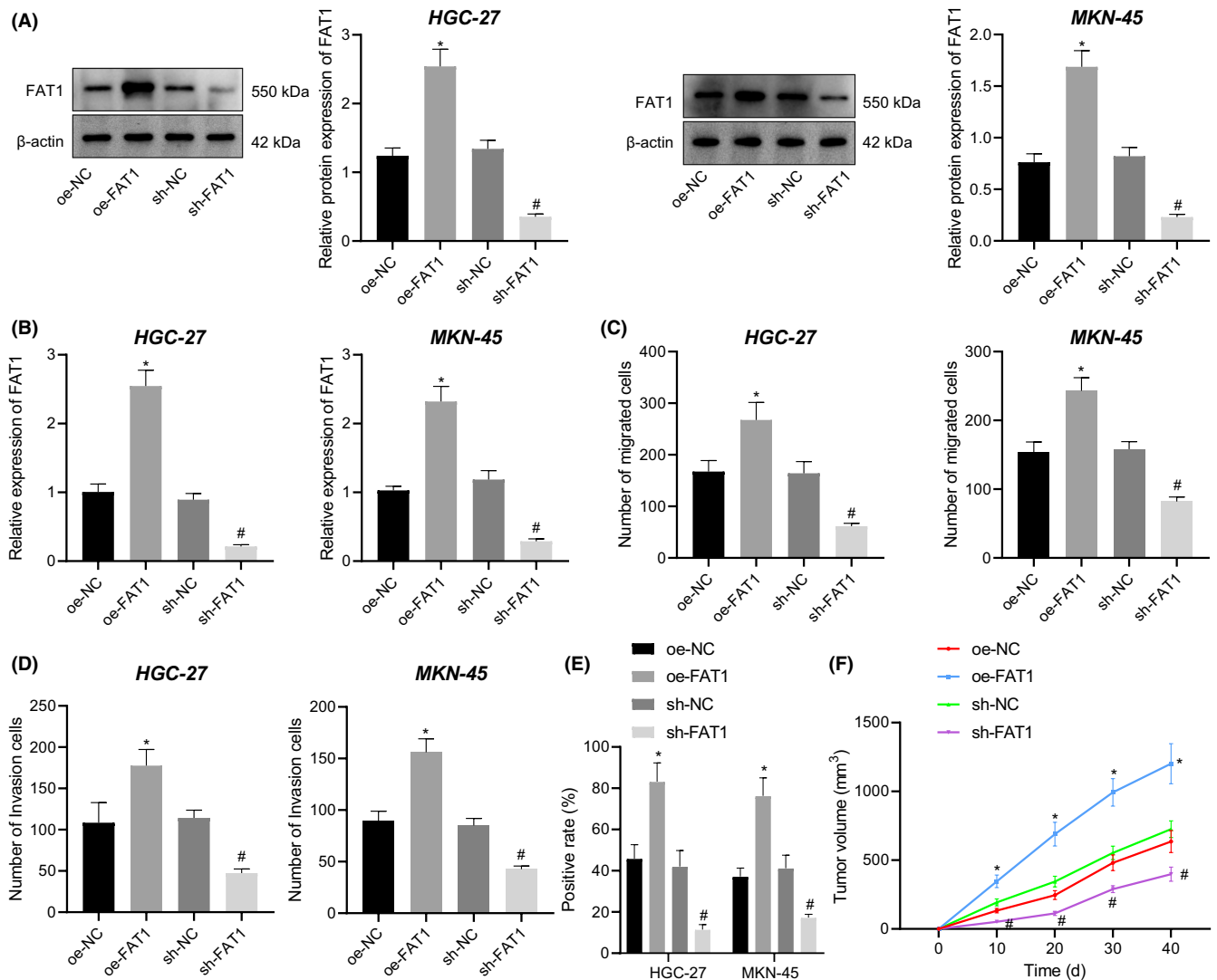
FIGURE 2 FAT1 promotes the proliferation, migration, invasion in vitro, and tumor growth in vivo of GC cells. (A) Transduction efficiency of oe-FAT1 and sh-FAT1 determined by western blot analysis in HGC-27 and MKN-45 cells. (B) Transduction efficiency of oe-FAT1 and sh-FAT1 determined by RT-qPCR in HGC-27 and MKN-45 cells. (C) Cell migration measured by Transwell assay in HGC-27 and MKN-45 cells upon transfection with oe-FAT1 or sh-FAT1. (D) Cell invasion measured by Transwell assay in HGC-27 and MKN-45 cells upon transduction with oe-FAT1 or sh-FAT1. (E) Cell proliferation measured by EdU assay in HGC-27 and MKN-45 cells upon transduction with oe-FAT1 or sh-FAT1. (F) Tumor volume of nude mice treated with oe-FAT1 or sh-FAT1 ($n = 6$). Data are shown as mean ± standard deviation. Cell experiments were repeated three times. Data among multiple groups were analyzed by one-way ANOVA, followed by a Tukey multiple comparisons posttest. The repeated measures ANOVA with Tukey's post hoc test was applied for the comparison of data at different time points. *$p < 0.05$, compared with HGC-27 and MKN-45 cells transfected with oe-NC. #$p < 0.05$, compared with HGC-27 and MKN-45 cells transfected with sh-NC

documented to modulate the activity of the key transcription factor AP-1.[12] Consistently, results of dual-luciferase reporter gene assay identified that overexpression of FAT1 promoted the transcriptional activity of AP-1, while knockdown of FAT1 led to inhibited AP-1 transcriptional activity (Figure 3A). The phosphorylation of c-Fos and c-Jun is a well established parameter of AP-1 transcriptional activity.[15] Through western blot analysis, FAT1 was revealed to upregulate AP-1 protein expression by promoting phosphorylation

levels of c-Jun and c-fos, and knocking down FAT1 led to the opposite results (Figure 3B). We then treated the cells with PNRI-299, a specific inhibitor of AP-1. As depicted in Figure 3C–E, PNRI-299 treatment abolished the promoting effect of FAT1 overexpression on the proliferative, migratory, and invasive functions of GC cells. These results supported the conclusion that FAT1 might upregulate AP-1 expression and therefore augmented the malignant behaviors of GC cells.
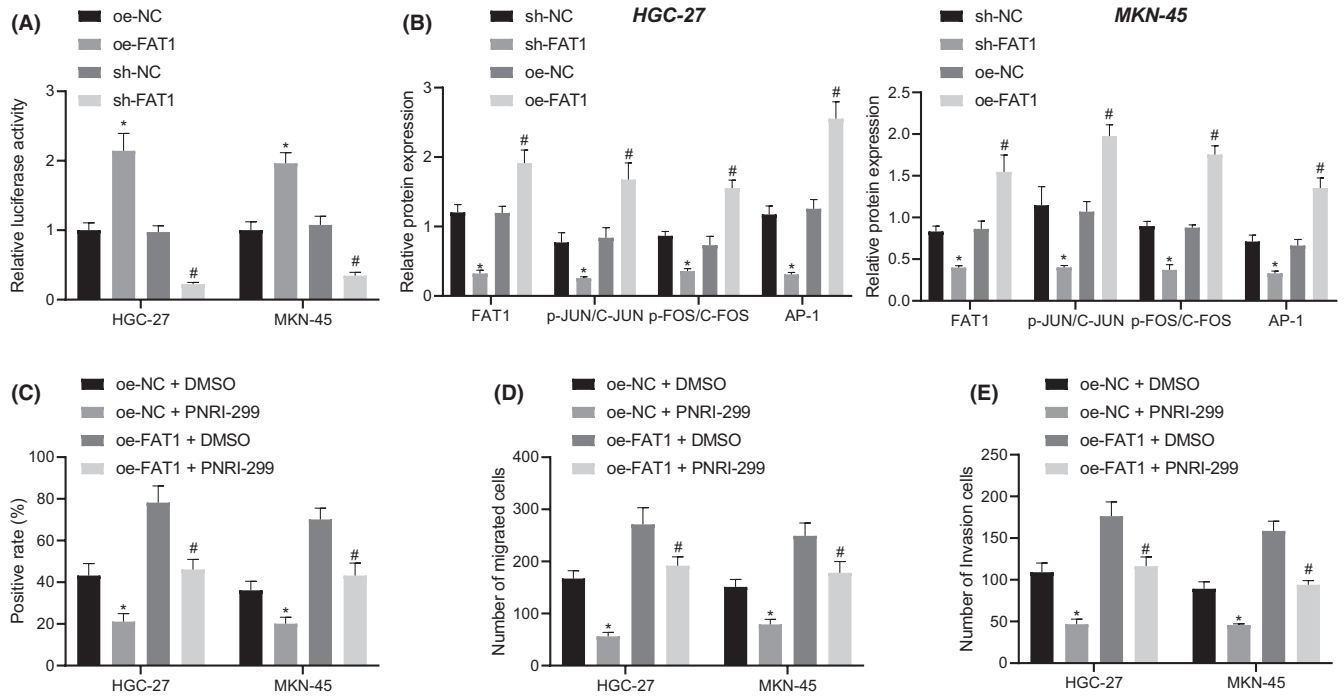
FIGURE 3 FAT1 increases AP-1 expression to stimulate the malignant characteristics of GC cells. (A) Transcriptional activity of AP-1 detected by dual-luciferase assay in HGC-27 and MKN-45 cells transduced with oe-FAT1 or sh-FAT1. (B) Western blot analysis of AP-1 protein in HGC-27 and MKN-45 cells transduced with oe-FAT1 or sh-FAT1. (C) HGC-27 and MKN-45 cell proliferation measured by EdU assay. (D) HGC-27 and MKN-45 cell migration measured by Transwell assay upon treatment with PNRI-299. (E) HGC-27 and MKN-45 cell invasion measured by Transwell assay upon treatment with PNRI-299. Data are shown as mean ± standard deviation. Cell experiments were repeated three times. Data among multiple groups were analyzed by one-way ANOVA, followed by a Tukey multiple comparisons posttest. *$p < 0.05$, compared with cells transduced with oe-NC, sh-NC or oe-NC + DMSO. #$p < 0.05$, compared with cells transduced with sh-NC, oe-NC or oe-FAT1 + DMSO

3.4 | TFAP2C upregulates the expression of FAT1 and therefore promotes the malignant characteristics of GC cells

Furthermore, to characterize the upstream mechanism of FAT1, we predicted the upstream transcription factors of FAT1 using the lnc-MAP database (http://bio-bigdata.hrbmu.edu.cn/LncMAP/gene-tf.jsp) (Table S3). Then we analyzed the interaction between the predicted transcription factors using the STRING database (https://string-db.org/), and constructed the gene interaction network diagram (Figure 4A). The figure shows complex regulatory networks in these transcription factors, among which TFAP2C has been associated with the super-enhancer in GC.[9] Additionally, TFAP2C had an interaction with many transcription factors in the network, and an enhancer regulatory region was found in the promoter region of FAT1 (Figure 4B). Moreover, JASPAR database-based analysis (http://jaspar.genereg.net/) suggested that FAT1 was regulated by TFAP2C (Table S4). TFAP2C expression was abundant in GC samples in TCGA and GTEx databases (Figure 4C). Here, we focused on TFAP2C in subsequent experiments.

The overexpression of TFAP2C was verified in clinically collected GC tissues ($n = 46$) relative to adjacent normal tissues ($n = 46$) (Figure 4D). Dual-luciferase reporter gene and ChIP assays verified the binding affinity of TFAP2C to the promoter region of

FAT1 (Figure 4E,F). Subsequently, HGC-27 cells were treated with oe-TFAP2C or sh-TFAP2C (Figure 4G). Upon overexpression of TFAP2C, the proliferative, migratory, and invasive abilities of GC cells were enhanced, all of which were suppressed in response to TFAP2C knockdown (Figure 4H,I).

These results indicated that TFAP2C could enhance the oncogenic phenotypes of GC cells by enhancing the transcription of FAT1.

3.5 | LINC00857 recruits TFAP2C to promote FAT1 gene expression, therefore boosting malignant characteristics of GC cells

Profiling of a GC-related expression microarray GSE19826 (including three normal samples and 12 tumor samples) revealed the high expression of LINC00857 in GC samples (Figure 5A). Furthermore, LINC00857 expression was amplified in GC samples included in TCGA and GTEx databases (Figure 5B). Bioinformatics analysis predicted the interaction between TFAP2C and LINC00857: prediction using RF classifier: 0.7; prediction using a support vector machine (SVM) classifier: 0.97 (Figure 5C).

In addition, LINC00857 and TFAP2C were co-located in the nucleus of GC cells (HGC-27 and MKN-450 and GES-1 cells, as revealed by FISH assay; Figure 5D). LINC00857 showed an
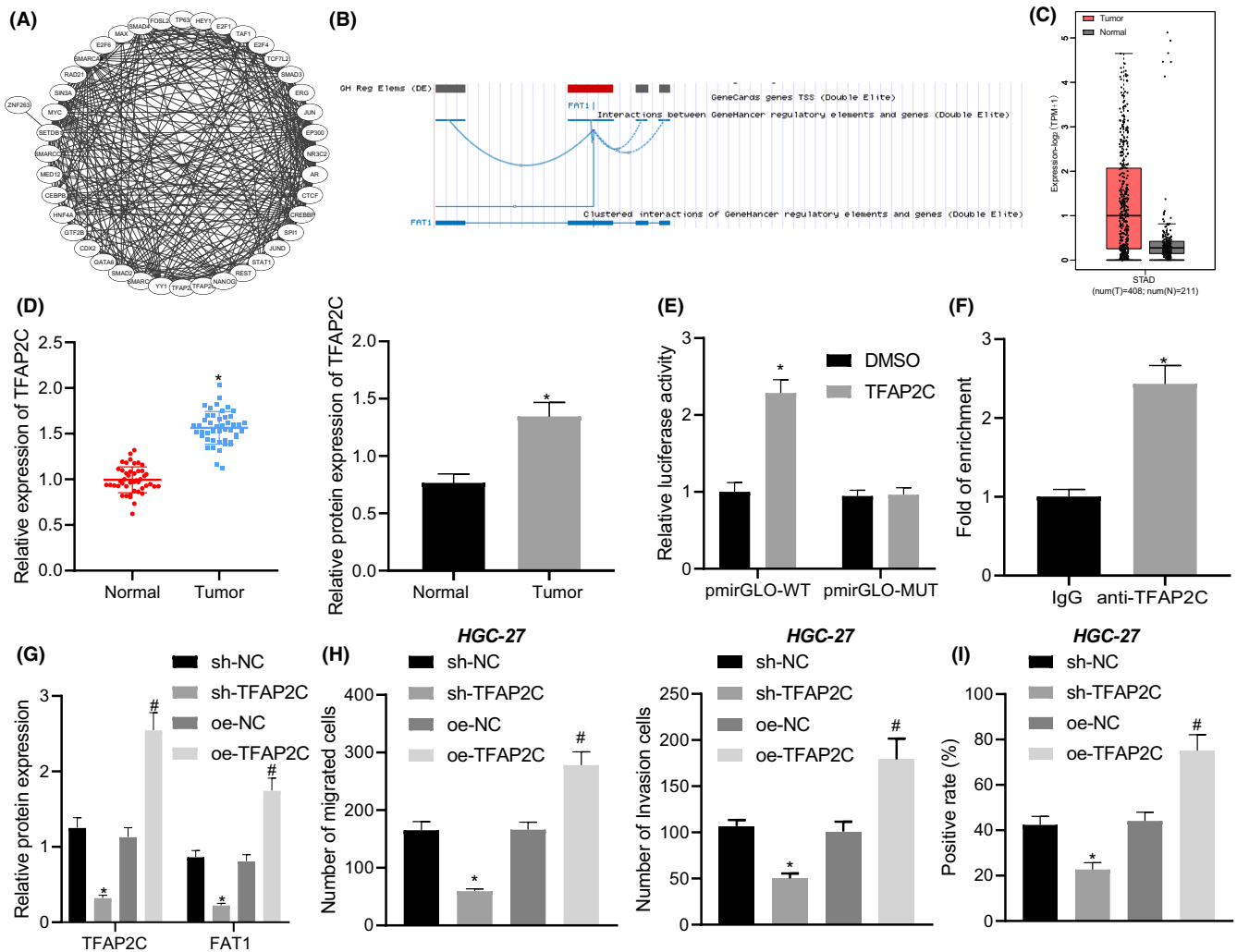
FIGURE 4 TFAP2C potentiates the malignant behaviors of GC cells by FAT1 upregulation. (A) Interaction network of upstream transcription factors of FAT1 in GC analyzed by the Cytoscape software (Cytoscape_v3.7.1). Each circle represents a gene, and the connection between circles indicates the interaction between genes. (B) Prediction of the super-enhancer in the FAT1 promoter region by UCSC database (http://genome.ucsc.edu/cgi-bin/hgTracks?hgsid=853606293_ra2O91bygP5w6iotXkmLSJDIBgMa). (C) Expression of TFAP2C in GC and normal samples included in TCGA and GTEX of the GEPIA2 database (http://gepia2.cancer-pku.cn/#analysis). (D) Expression of TFAP2C in GC ($n = 46$) and adjacent normal tissues ($n = 46$) determined by RT-qPCR and western blot analysis. (E) Binding of TFAP2C to the FAT1 promoter assessed by dual-luciferase reporter gene assay. (F) Interaction between TFAP2C and the FAT1 promoter assessed by ChIP assay. (G) Transduction efficiency of oe-TFAP2C or sh-TFAP2C determined by western blot analysis in HGC-27 cells. (H) HGC-27 cell migration and invasion measured by Transwell assays upon transduction with oe-TFAP2C or sh-TFAP2C. (I) HGC-27 cell proliferation measured by EdU assay upon transduction with oe-TFAP2C or sh-TFAP2C. Data are shown as mean±standard deviation. Cell experiments were repeated three times. Data between two groups were compared with unpaired t-test while those among multiple groups were analyzed by one-way ANOVA, followed by a Tukey multiple comparisons posttest. *$p < 0.05$, compared with normal samples, DMSO-treated HGC-27 cells, IgG antibody or sh-NC-transfected HGC-27 cells. #$p < 0.05$, compared with MKN-45 cells transduced with oe-NC

interplay with TFAP2C, as demonstrated by RIP assay (Figure 5E). In addition, RNA pull-down assay also verified their interaction (Figure 5F,G). Furthermore, LINC00857 and TFAP2C expression was manipulated in HGC-27 cells. When LINC00857 was knocked down, FAT1 expression was decreased, whereas TFAP2C restoration reversed this decrease (Figure 5H). In the presence of LINC00857 knockdown, the migration, invasion, and proliferation of GC cells were attenuated, yet simultaneous TFAP2C overexpression relatively negated the effects of LINC00857 knockdown (Figure 5I–J).

The aforementioned results suggested that LINC00857 may recruit TFAP2C to promote FAT1 gene expression, thereby potentiating phenotypes of GC cells.

3.6 | LINC00857 knockdown impedes tumor growth in vivo

Next, we performed in vivo experiments to verify the relationship between LINC00857 and the TFAP2C/FAT1/AP-1 signaling axis and
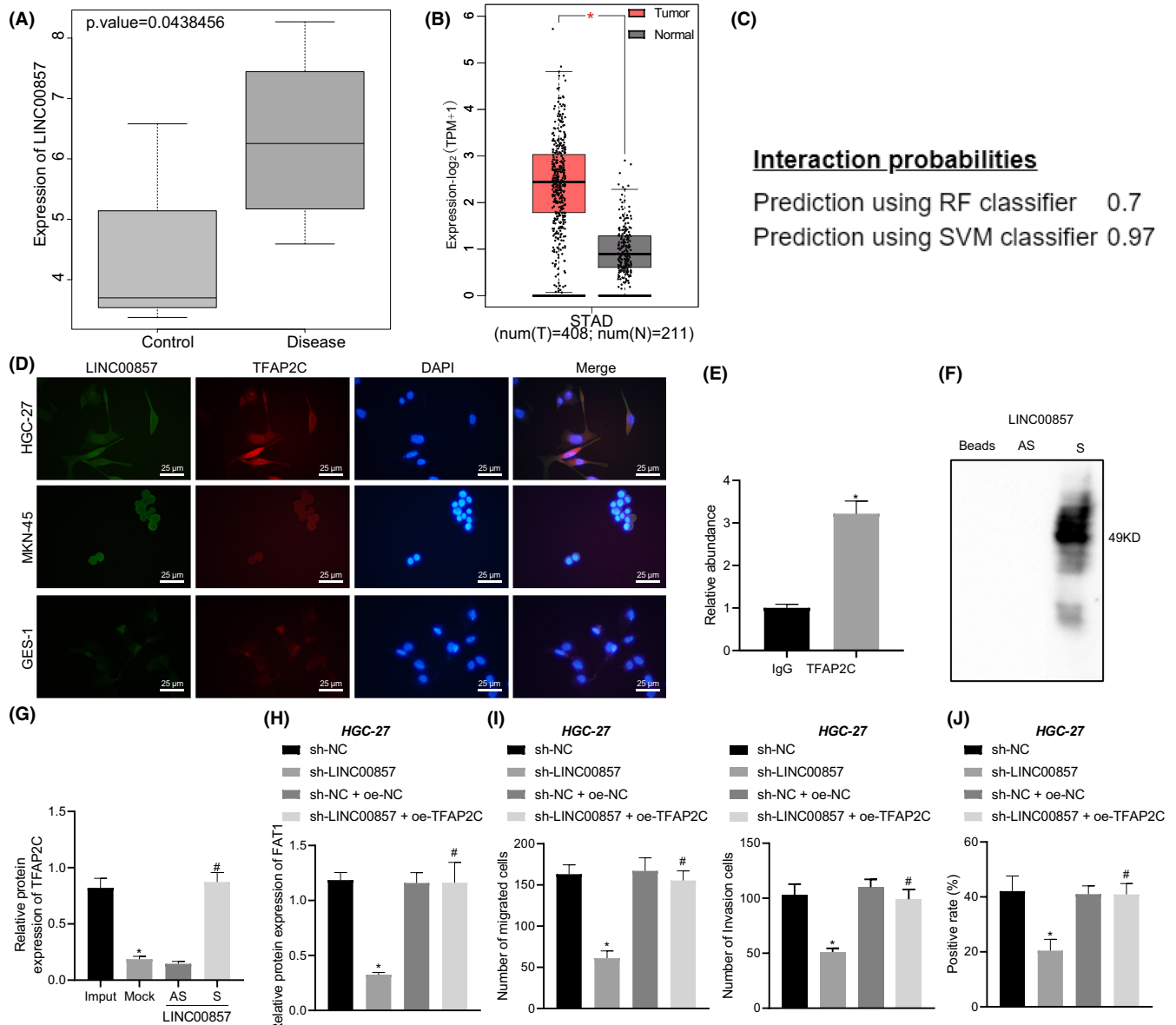
FIGURE 5 LINC00857 recruits TFAP2C to promote FAT1 gene expression, therefore promoting the malignant characteristics of GC cells. (A) LINC00857 expression in the GSE19826 data set from the GEO database (https://www.ncbi.nlm.nih.gov/geo/). The abscissa represents the sample type, the ordinate represents the expression value, the left box diagram represents the normal sample, the right box diagram represents the disease sample, and the upper left corner is the *p*-value. (B) LINC00857 expression in GC and normal samples included in TCGA and GTEx of the GEPIA2 database (http://gepia2.cancer-pku.cn/#analysis). * *p* < 0.01. (C) Interaction of TFAP2C and LINC00857 analyzed by an online tool (http://pridb.gdcb.iastate.edu/RPISeq/results.php). Interaction probabilities of RPISeq range from 0 to 1. In terms of performance evaluation, predictions with probabilities >0.5 were considered "positive," indicating that the corresponding RNA and protein are likely to interact. (D) Co-localization of TFAP2C and LINC00857 evaluated by FISH assay and immunofluorescence staining in GC cells (HGC-27 and MKN-450 and GES-1 cells) (LINC00857 in green, TFAP2C protein in red, DAPI-stained nuclei in blue). (E) Interaction of TFAP2C and LINC00857 determined by RIP assay. (F) Interaction of TFAP2C and LINC00857 determined by RNA pull-down assay. S, sense; AS, antisense. (G) The interaction between TFAP2C and LINC00857 determined by RNA pull-down assay. S, sense; AS, antisense (H) Western blot analysis of FAT1 protein in HGC-27 cells upon LINC00857 knockdown alone or in combination with TFAP2C overexpression. (I) HGC-27 cell migration and invasion measured by Transwell assay upon LINC00857 knockdown alone or in combination with TFAP2C overexpression. (J) HGC-27 cell proliferation measured by EdU assay upon LINC00857 knockdown alone or in combination with TFAP2C overexpression. Data are shown as mean ± standard deviation. Cell experiments were repeated three times. Data between two groups were compared using unpaired *t*-test, whereas those among multiple groups were analyzed by one-way ANOVA, followed by a Tukey multiple comparisons posttest. *p < 0.05, compared with IgG antibody, sh-NC-transfected HGC-27 cells, or input. #p < 0.05, compared with HGC-27 cells transduced with sh-LINC00857 or AS group
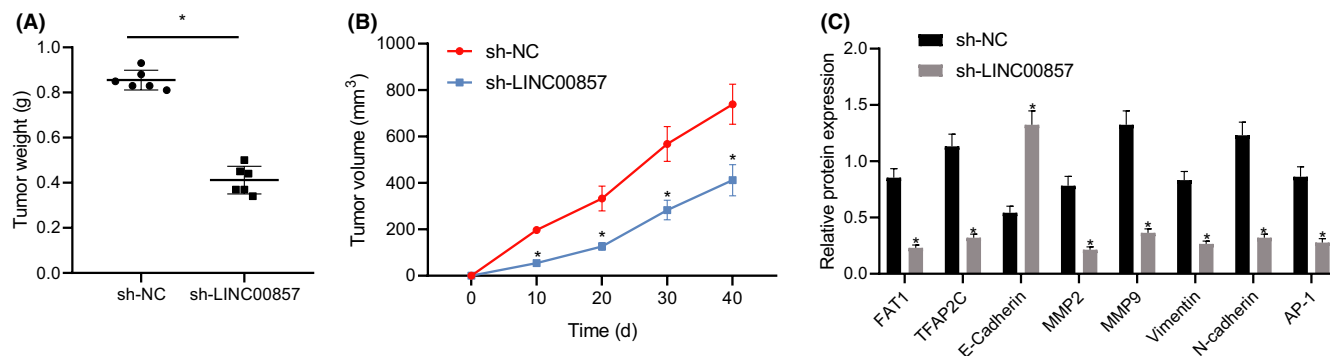
FIGURE 6 LINC00857 knockdown retards the tumor growth in nude mice. (A) Weight of GC xenografted tumors of mice treated with sh-LINC00857. (B) Tumor volume of mice treated with sh-LINC00857. (C) Western blot analysis of FAT1, TFAP2C, E-cadherin, MMP2, MMP9, Vimentin, N-cadherin, and AP-1 proteins in tumor tissues of mice treated with sh-LINC00857. $n = 6$. Data are shown as mean ± standard deviation. Data between two groups were compared with unpaired t-test while those among multiple groups at varied time points were analyzed by repeated measures ANOVA, followed by Tukey multiple comparisons post test. *$p < 0.05$, compared with mice treated with sh-NC

identify their effects on tumor growth. The body weight of nude mice exhibited no alterations in control and sh-LINC00857-treated mice (Figure 6A), while tumor growth was inhibited following knockdown of LINC00857 (Figure 6B). At the same time, the expression of FAT1, TFAP2C, N-cadherin, MMP2, MMP9 and vimentin was downregulated, whereas that of E-cadherin was upregulated in mouse tumor tissues (Figure 6C). Therefore, knockdown of LINC00857 could inhibit tumor growth in vivo by inhibiting the activation of the TFAP2C/FAT1 signaling axis.

4 | DISCUSSION

In this study, we explored the potential role of FAT1 in GC as well as the possible upstream and downstream molecular mechanisms. Our results suggested that LINC00857 recruited TFAP2C to enhance its transcription, and consequently upregulated FAT1 and AP-1 expression, ultimately accelerating GC cell malignant phenotypes.

FAT1 acts as a tumor suppressor or oncogene in a context-dependent manner.[16] This study identified the upregulated FAT1 expression n GC tissues and cells, which showed a correlation with the pathological grade of GC patients. In addition, FAT1 was also found to stimulate the proliferative, migratory and invasive property of GC cells in vitro. Consistently, FAT1 expression was upregulated in GC tissues and, conversely, its silencing could suppress cell migration and invasion abilities; patients with high FAT1 expression had a poor prognosis.[11]

FAT1 knockdown by siRNA can result in increased expression of the PDCD4 gene, which in turn leads to the attenuation of AP-1 transcription by inhibiting the phosphorylation level of c-Jun.[12] Jun is known as a subunit of AP-1.[17] It could be therefore hypothesized that FAT1 could upregulate AP-1 expression by promoting phosphorylation levels of c-Jun, which was in accordance our findings. At the same time, inhibiting the transcription factor AP-1 by ADRB2 antagonists has the potential to suppress the proliferative
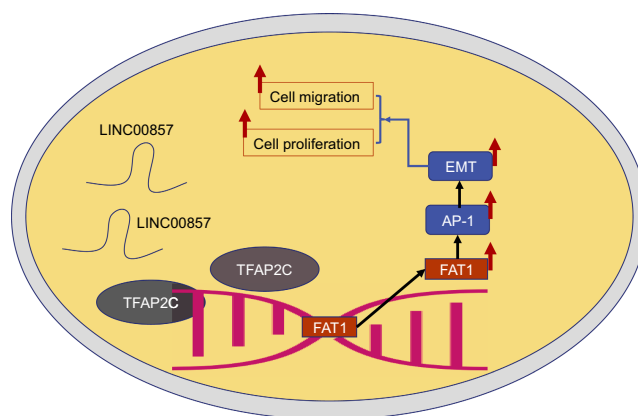

FIGURE 7 The graphical summary of the function and mechanism of LINC00857 in GC. LINC00857 recruits TFAP2C to promote its transcription, therefore enhancing FAT1 and AP-1 expression, ultimately contributing to the progression of GC

and metastatic capacities of GC cells.[18] Also, AP-1 knockdown can inhibit the resistance of GC cells to chemotherapy.[19] Therefore, it can be concluded that FAT1 might upregulate AP-1 expression and therefore augmented the malignant characteristics of GC cells.

TFAP2C is a GC-related gene and found to be potentially methylated in primary GC.[20] In addition, TFAP2C has association with the super-enhancer in GC.[8] TFAP2C is abundantly expressed in tissues and cells of colorectal cancer and enhances spheroids formation ability in vitro[9]. The present study revealed that TFAP2C could promote migration, invasion, and proliferation of GC cells by enhancing the transcription of the FAT1 gene. However, due to the lack of available literature, the established interaction between TFAP2C and FAT1, and the TFAP2C promoting properties on the malignant characteristics of GC cells are still required to be further exploited.

Additionally, the current results demonstrated that LINC00857 could recruit TFAP2C to promote FAT1 gene expression, therefore

boosting the malignant characteristics of GC cells. Compared with GES-1 cell line, an approximately two-fold upregulated expression for the LINC00857 has been observed in GC cell lines.[6] In addition, overexpression of LINC00857 exhibited a positive correlation with the tumor size of patients with GC, whereas the siRNA-mediated LINC00857 knockdown impeded the proliferative potential of GC cells.[21] More importantly, silencing of LINC00857 can enhance the EMT process, supported by increased E-cadherin and repressed N-cadherin protein, thereby restraining hepatocellular carcinoma cell migration and invasion capacity.[22] Our data revealed the interaction between TFAP2C and LINC00857 when LINC00857 could recruit TFAP2C. Furthermore, silencing of LINC00857 diminished FAT1 expression, revealed by western blot analysis, whereas further studies are also warranted owing to the little progress made in their relationship. However, accumulating data have shown the controlling of lncRNAs in their downstream AP-1, therefore being involved in the progression of human cancers.[23,24] Partially in agreement with the above, LINC00857 knockdown was found to impair tumor growth through disruption of the TFAP2C/FAT1/AP-1 signaling axis.

In conclusion, LINC00857 may recruit TFAP2C to promote its transcription, and therefore potentiates the FAT1 and AP-1 expression, ultimately accelerating the progression of GC (Figure 7). The newly found LINC00857/TFAP2C/FAT1/AP-1 network sheds new light on the mechanism underlying the carcinogenesis of GC. These findings might well aid in the development of intervention strategies for GC. However, further studies are warranted to elucidate the specific mechanisms behind the established axis to a pending more detailed validation eventually contributing to clinical applications.

ACKNOWLEDGMENTS
None.

AUTHOR CONTRIBUTIONS
WQZ, KYJ, CCM, CPZ, and LY participated in the conception and design of the study. WQZ, KYJ, CCM, CPZ, LY, and QZ performed the analysis and interpretation of data. CCM, ZBT, and MYZ contributed to drafting the article. WQZ, KYJ, QZ, and XYL revised it critically for important intellectual content. XYL is the GUARANTOR for the article who accepts full responsibility for the work and/or the conduct of the study, had access to the data, and oversaw the decision to publish.

DISCLOSURE
The authors have no conflict of interest.

ORCID
Xiaoyu Li https://orcid.org/0000-0001-8017-207X

REFERENCES
1. Karimi P, Islami F, Anandasabapathy S, Freedman ND, Kamangar F. Gastric cancer: descriptive epidemiology, risk factors, screening, and prevention. *Cancer Epidemiol Biomarkers Prev*. 2014;23:700-713.
2. Smyth EC, Nilsson M, Grabsch HI, van Grieken NC, Lordick F. Gastric cancer. *Lancet*. 2020;396:635-648.
3. Chen W, Zheng R, Baade PD, et al. Cancer statistics in China, 2015. *CA Cancer J Clin*. 2016;66:115-132.
4. Cancer Genome Atlas Research N. Comprehensive molecular characterization of gastric adenocarcinoma. *Nature*. 2014;513:202-209.
5. Gu Y, Chen T, Li G, et al. LncRNAs: emerging biomarkers in gastric cancer. *Future Oncol*. 2015;11:2427-2441.
6. Zhang K, Shi H, Xi H, et al. Genome-wide lncRNA microarray profiling identifies novel circulating lncRNAs for detection of gastric cancer. *Theranostics*. 2017;7:213-227.
7. Pastor WA, Liu W, Chen D, et al. TFAP2C regulates transcription in human naive pluripotency by opening enhancers. *Nat Cell Biol*. 2018;20:553-564.
8. Ooi WF, Xing M, Xu C, et al. Epigenomic profiling of primary gastric adenocarcinoma reveals super-enhancer heterogeneity. *Nat Commun*. 2016;7:12983.
9. Wang X, Sun D, Tai J, et al. TFAP2C promotes stemness and chemotherapeutic resistance in colorectal cancer via inactivating hippo signaling pathway. *J Exp Clin Cancer Res*. 2018;37:27.
10. Katoh Y, Katoh M. Comparative integromics on FAT1, FAT2, FAT3 and FAT4. *Int J Mol Med*. 2006;18:523-528.
11. Kang MH, Jeong GS, Smoot DT, et al. Verteporfin inhibits gastric cancer cell growth by suppressing adhesion molecule FAT1. *Oncotarget*. 2017;8:98887-98897.
12. Dikshit B, Irshad K, Madan E, et al. FAT1 acts as an upstream regulator of oncogenic and inflammatory pathways, via PDCD4, in glioma cells. *Oncogene*. 2013;32:3798-3808.
13. Zhu G, Ye J, Huang Y, et al. Receptor-interacting protein-1 promotes the growth and invasion in gastric cancer. *Int J Oncol*. 2016;48:2387-2398.
14. Sun Y, He J, Shi DB, et al. Elevated ZBTB7A expression in the tumor invasive front correlates with more tumor budding formation in gastric adenocarcinoma. *J Cancer Res Clin Oncol*. 2021;147:105-115.
15. Cai WT, Guan P, Lin MX, Fu B, Wu B. Sirt1 suppresses MCP-1 production during the intervertebral disc degeneration by inactivating AP-1 subunits c-Fos/c-Jun. *Eur Rev Med Pharmacol Sci*. 2020;24:5895-5904.
16. Katoh M. Function and cancer genomics of FAT family genes (review). *Int J Oncol*. 2012;41:1913-1918.
17. Liu B, Zhang Y, Fan Y, et al. Leucine-rich repeat neuronal protein-1 suppresses apoptosis of gastric cancer cells through regulation of Fas/FasL. *Cancer Sci*. 2019;110:2145-2155.
18. Zhang X, Zhang Y, He Z, et al. Chronic stress promotes gastric cancer progression and metastasis: an essential role for ADRB2. *Cell Death Dis*. 2019;10:788.
19. Yang W, Zhao S, Wu B, et al. BATF2 inhibits chemotherapy resistance by suppressing AP-1 in vincristine-resistant gastric cancer cells. *Cancer Chemother Pharmacol*. 2019;84:1279-1288.

20. Yamashita S, Tsujino Y, Moriguchi K, Tatematsu M, Ushijima T. Chemical genomic screening for methylation-silenced genes in gastric cancer cell lines using 5-aza-2′-deoxycytidine treatment and oligonucleotide microarray. *Cancer Sci*. 2006;97:64-71.

21. Pang K, Ran MJ, Zou FW, Yang TW, He F. Long non-coding RNA LINC00857 promotes gastric cancer cell proliferation and predicts poor patient survival. *Oncol Lett*. 2018;16:2119-2124.

22. Xia C, Zhang XY, Liu W, et al. LINC00857 contributes to hepatocellular carcinoma malignancy via enhancing epithelial-mesenchymal transition. *J Cell Biochem*. 2019;120:7970-7977.

23. Jiang R, Tang J, Chen Y, et al. The long noncoding RNA lnc-EGFR stimulates T-regulatory cells differentiation thus promoting hepatocellular carcinoma immune evasion. *Nat Commun*. 2017;8:15129.

24. Ji J, Yin Y, Ju H, et al. Long non-coding RNA Lnc-Tim3 exacerbates CD8 T cell exhaustion via binding to Tim-3 and inducing nuclear translocation of Bat3 in HCC. *Cell Death Dis*. 2018;9:478.

SUPPORTING INFORMATION

Additional supporting information can be found online in the Supporting Information section at the end of this article.